

Henry Ford Health

## Henry Ford Health Scholarly Commons

---

Research Articles

Research Administration

---

9-1-2021

### rsfMRI based evidence for functional connectivity alterations in adults with developmental stuttering

Seyedehsamaneh Shojaeilangari

Narges Radman

Mohammad Ehsan Taghizadeh

Hamid Soltanian-Zadeh

*Henry Ford Health*, Hsoltan1@hfhs.org

Follow this and additional works at: [https://scholarlycommons.henryford.com/research\\_articles](https://scholarlycommons.henryford.com/research_articles)

---

#### Recommended Citation

Shojaeilangari S, Radman N, Taghizadeh ME, and Soltanian-Zadeh H. rsfMRI based evidence for functional connectivity alterations in adults with developmental stuttering. *Heliyon* 2021; 7(9):e07855.

This Article is brought to you for free and open access by the Research Administration at Henry Ford Health Scholarly Commons. It has been accepted for inclusion in Research Articles by an authorized administrator of Henry Ford Health Scholarly Commons.



## Research article

## rsfMRI based evidence for functional connectivity alterations in adults with developmental stuttering

Seyedehsamaneh Shojaeilangari<sup>a,\*</sup>, Narges Radman<sup>a,b</sup>, Mohammad Ehsan Taghizadeh<sup>c</sup>, Hamid Soltanian-Zadeh<sup>a,d,e</sup><sup>a</sup> School of Cognitive Science, Institute for Research in Fundamental Sciences (IPM), P.O. Box 1954851167, Tehran, Iran<sup>b</sup> Department of Psychiatry, Tehran University of Medical Sciences, Tehran, Iran<sup>c</sup> Department of Psychology, Payame Noor University, Tehran, Iran<sup>d</sup> CIPCE, School of Electrical and Computer Engineering, College of Engineering, Tehran University, Tehran, Iran<sup>e</sup> Departments of Radiology and Research Administration, Henry Ford Health System, Detroit, Michigan, USA

## ARTICLE INFO

## Keywords:

Persistent developmental stuttering (PDS)  
Functional connectivity  
Resting state functional magnetic resonance imaging (fMRI)

## ABSTRACT

Persistent developmental stuttering (PDS) is defined as a speech disorder mainly characterized by intermittent involuntary disruption in normal fluency, time patterning, and rhythm of speech. Although extensive functional neuroimaging studies have explored brain activation alterations in stuttering, the main affected brain regions/networks in PDS still remain unclear. Here, using functional magnetic resonance imaging (fMRI), we investigated resting-state whole-brain functional connectivity of 15 adults who stutter (PDS group) and 15 age-matched control individuals to reveal the connectivity abnormalities associated with stuttering. We were also interested in exploring how the severity of stuttering varies across individuals to understand the compensatory mechanism of connectivity pattern in patients showing less symptoms. Our results revealed decreased connectivity of left frontal pole and left middle frontal gyrus (MidFG) with right precentral/postcentral gyrus in stuttering individuals compared with control participants, while less symptomatic PDS individuals showed greater functional connectivity between left MidFG and left caudate. Additionally, our finding indicated reduced connectivity in the PDS group between the left superior temporal gyrus (STG) and several brain regions including the right limbic lobe, right fusiform, and right cerebellum, as well as the left middle temporal gyrus (MTG). We also observed that PDS individuals with less severe symptoms had stronger connectivity between right MTG and several left hemispheric regions including inferior frontal gyrus (IFG) and STG. The connectivity between right fronto-orbital and right MTG was also negatively correlated with stuttering severity. These findings may suggest the involvement of right MTG and left MidFG in successful compensatory mechanisms in more fluent stutterers.

## 1. Introduction

The interest in investigating the affected neural mechanisms in neurological and psychiatric disorders is growing fast. In these areas, clinicians rely on therapeutic approaches, which are based on empirical observations with limited knowledge about the underlying mechanisms in the brain. Yet knowledge about the neural basis underlying the behavioral amendment of disorders could help improve the therapies.

Stuttering is a speech disorder mainly characterized by repeated sounds or syllables or even words, intermittent prolongations and blocks, and disruptions in normal speech rate often accompanied by physical tension. Stuttering is categorized into three types including

developmental, neurogenic, and psychogenic [1]. Developmental stuttering (DS) is very common in children under five, as children are developing their language abilities. Approximately 5% of children experience this type of stuttering, which usually resolves naturally without any therapeutic intervention. Only 1% of DS children (mostly boys) will have it persist through adulthood [2]. Indeed, persistent DS (PDS) is a form of DS that has not remitted spontaneously or by any treatment [1]. Stuttering has a significant adverse impact on overall quality of life where it affects psychological health through increasing the rate of social anxiety, educational underachievement, and reduced social wellbeing.

\* Corresponding author.

E-mail address: [s.shojaei@ipm.ir](mailto:s.shojaei@ipm.ir) (S. Shojaeilangari).<https://doi.org/10.1016/j.heliyon.2021.e07855>

Received 13 April 2021; Received in revised form 28 May 2021; Accepted 19 August 2021

2405-8440/© 2021 The Author(s). Published by Elsevier Ltd. This is an open access article under the CC BY-NC-ND license (<http://creativecommons.org/licenses/by-nc-nd/4.0/>).

Although the cause of stuttering is unknown, the underlying nature of the disorder appears to involve a genetic susceptibility that is neurologically expressed as abnormalities in brain structure and function [3]. Over the past few decades, neuroimaging techniques such as MRI/fMRI, EEG, MEG, and PET have greatly contributed to the discovery of neural bases of stuttering [4].

Task based fMRI researches have revealed the contribution of a number of brain regions such as cerebellum, basal ganglia, auditory cortex, premotor/motor areas, and speech related regions to stuttering [5, 6]. However, such a task induced neuroimaging outcomes may be confounded by speech production artifacts. This issue can be overcome by using resting-state fMRI (rsfMRI); an advanced neuroimaging technique to gain the knowledge of neurophysiological mechanisms by measuring brain activity in the absence of any explicit task or stimuli while the subject is at rest [7, 8, 9].

Xuan et al. [2] have studied the brain activity of 44 adults with DS and 46 fluent controls by an extensive analysis of rsfMRI measures such as amplitude of low-frequency fluctuation (ALFF) metric, region of interest (ROI)-based functional connectivity (FC), and independent component analysis (ICA)-based FC. It is reported that compared to control subjects, PDS patients showed higher ALFF in several brain areas involved in motor, language, and auditory processing, as well as cognitive function, but reduced ALFF in bilateral supplementary motor area (SMA). Moreover, based on ROI analysis, they showed reduced FC between the posterior language reception area and anterior brain regions related to initiation of speech motor, but increased FC within anterior/posterior speech associated regions in the PDS group. ICA analysis also revealed an increased FC in the sensorimotor network in stuttering subjects.

Yang et al. [5] using rsfMRI of 16 stutters and 18 controls and seed-to-voxel analysis demonstrated alternations in FC between cerebellum and motor cortex, as well as connectivity among different loci within cerebellum for PDS. They reported decreased connectivity between the basal ganglia and right SMA, as well as bilateral STG, but increased connectivity between the cerebellum and right IFG which was positively correlated with the stuttering severity. Lu et al. [10] investigated the resting-state FC (RSFC) and cortical thickness alterations in PDS before and after a short term intervention (15 stuttering patients who received the intervention, 13 stuttering patients who did not take the intervention, and 13 control subjects). They reported significant reductions of FC and cortical thickness in left pars-opercularis but increases in the cerebellum for PDS before intervention compared to the control group. Moreover, they showed that the intervention decreased stuttering by FC reduction in the cerebellum to the level of controls.

Lu et al. [11] further examined the relation between speech perception and production in 13 PDS subjects compared to 13 controls using both perception task and rsfMRI data. The authors found an association between speech perception impairment and anomalous functional activity in the speech motor area and also the impaired FC between this area and auditory region in stuttering subjects. Desai et al. [12] used perfusion MRI to investigate the resting cerebral blood flow (rCBF) in children/adults who stutter (26 stutterers and 36 controls). They reported a reduced CBF in Broca's region that was correlated with stuttering severity symptoms. Since this was also observed in stuttering children, the authors related this finding to the stuttering pathophysiology.

Overall, the literature shows that there are widespread functional and structural brain differences between adults/children who stutter and their fluent peers, although the pattern of observed results across different studies remains inconsistent [13]. What we can conclude based on the neuroimaging studies on PDS is that individuals with PDS present subtle structural and functional changes involving left-hemispheric brain regions that support fluent speech production. This includes areas in the left frontal cortex such as IFG which controls speech planning or motor cortex which plays an important role in speech execution [14], as well as auditory sensory regions located in the temporal lobe, i.e., Brodmann areas 41 and 42, which are involved in the sensory feedback of speech

sounds [15]. There is also evidence of the relationship between stuttering and alterations in deeper brain regions including cerebellum, thalamus, and basal ganglia, which support speech movements coordination by providing internal timing cues and motor sequencing control [5]. New findings about the neural underpinnings of PDS may result in new approaches that would improve the efficacy of speech therapies that maximize brain plasticity resulting in producing more fluent speech.

In this work, using rsfMRI, we investigated the RSFC of 15 adults who suffer from PDS and 15 age-matched control participants. Using a seed-driven FC analysis, we decided to evaluate the dynamic interaction of the main regions involved in language perception and production with the whole brain in the resting state. Our aim was to identify all regions that might have different connectivity patterns between PDS and healthy individuals in all brain regions. To this end, inspired by previous researches [13], we explored the seed regions located in the cerebellum, basal ganglia, frontal lobe, temporal lobe, and parietal lobe.

In addition to between group analyses, we were also interested to explore how the severity of stuttering varies across individuals. This helps to investigate and highlight compensatory connectivity patterns in less symptomatic PDS.

## 2. Method

### 2.1. Participants

Thirty participants were recruited in this study: 15 PDS (13 males and 2 females; mean age 27.8, age range 21–41) and a group of 15 age, sex, and education matched healthy controls (13 males and 2 females; mean age 25.66, age range 20–36). Demographic information of participants is shown in Table 1. All PDS subjects began to stutter in preadolescence ages and received no treatment during the year prior to this study. The severity of stuttering ranged from very mild to very severe (scored 0 to 100) based on Stuttering Severity Instrument-3 (SSI3) [16, 17] and Diagnostic and Statistical Manual of Mental Disorders (DSM-5) criteria [18].

The participants for this study were selected as physically healthy with no history of neurological diseases or mental illnesses based on their declaration. A safety questionnaire of the fMRI data acquisition was filled in to ensure the absence of contraindications of MRI recording. All of our participants were native Persian speakers from Iran, and checked to be right-handed as evaluated by the Edinburgh handedness inventory [19]. All subjects signed an informed consent prior to the experiment. The local ethical committee at the *Institute for Research in Fundamental Sciences (IPM)* approved the protocol of this study.

### 2.2. Image acquisition

MR images have been acquired on a Siemens Prisma 3.0 T MRI scanner at the National Brain Mapping Lab, Tehran, Iran. For each participant, foam pads and also fitted earplugs were used to limit the

**Table 1.** Demographic information of the participants.

Measures	Stuttering	Control	Group Difference (t-test)
	Mean (SD)	Mean (SD)	
Number of cases	15	15	NA
Sex	13 Male, 2 Female	13 Male, 2 Female	NA
Age	27.87 (5.60)	25.66 (4.47)	0.24 (NS)
TIV	1526.33 (98.87)	1525.33 (141.89)	0.98 (NS)
Stuttering Severity	79.44 (18.10)	NA	NA

Independent-sample t-test was used; TIV = total intracranial volume; SD = standard deviation; NA = not applicable; NS = not significant.

head movements and scanner noise respectively. Eight minutes of rsfMRI data was collected using a Blood Oxygen Level-Dependent (BOLD)-sensitive gradient echo-plane-image (EPI) sequence. Scan parameters were set as follows: echo time = 30 ms; repetition time = 2000 ms; flip angle = 90°; resolution =  $3 \times 3 \times 3 \text{ mm}^3$ ; field of view =  $195 \times 195 \text{ mm}^3$ ; and matrix size =  $384 \times 384$ . Each brain volume contained 34 contiguous axial slices, and each functional run contained 245 volumes. During the fMRI scan, all participants were asked to relax, keep their eyes closed, and avoid any movement. Sagittal three-dimensional T1-weighted images with a  $1 \times 1 \times 1 \text{ mm}^3$  resolution were acquired as well using a magnetization prepared rapid gradient echo (MP-RAGE) sequence (repetition time = 1810 ms; echo time = 3.470 ms; flip angle = 7°; matrix size =  $256 \times 256$ ).

### 2.3. Data analysis

Image preprocessing and statistical analysis have been done using CONN v.19c (<https://web.conn-toolbox.org/>) and SPM12 (<http://www.fil.ion.ucl.ac.uk/spm/>) toolboxes following a standard analysis pipeline [20].

For preprocessing, functional data were first realigned using SPM12, where all scans were coregistered and resampled to the first scan as a reference image. The field inhomogeneity inside the scanner (fieldmap) was also estimated from a double-echo sequence and used for Susceptibility Distortion Correction (SDC). Then, based on the slice-timing correction (STC) technique [21], temporal misalignment between slices of the functional data was corrected. Anatomical and functional data were next normalized into standard MNI space (Montreal Neurological Institute stereotactic space) with a resolution of  $1 \times 1 \times 1 \text{ mm}^3$  cubic voxels and segmented into grey matter, white matter, and cerebrospinal fluid (CSF). Last, for improving the signal-to-noise ratio (SNR), functional data were spatially smoothed using an isotropic Gaussian kernel with full width at half maximum (FWHM) of 8 mm. We also performed an extra experiment to check the effect of spatial smoothing on connectivity patterns by reducing the smoothing kernel size to 6 mm.

After preprocessing, to determine and remove the confounds in BOLD signal including noise components from white matter and CSF areas, as well as subject's estimated motion parameters, the CompCor strategy [22] was applied. The images were then band-pass filtered to 0.008–0.09 Hz to diminish the effect of noises from physiological processes, head-motion, and other sources.

For FC analysis [23], we used the seed-voxel correlation procedure to estimate the correlation of spontaneous BOLD activity between a pre-defined seed and remaining voxels of the brain. In other words, for seed-driven RSFC analysis, Pearson's bivariate correlation coefficients were calculated between the BOLD signal of a selected source seed ROI (averaged over all voxels within the ROI) and the time course of all other voxels. The measures were then converted to normally distributed scores using Fisher z-transformation for each participant to be ready for a second-level General Linear Model (GLM) based analysis. Finally, the functional connectivity maps of the participants were subsequently subjected into random effects analysis for group difference comparison using one-tailed two-sample *t*-test.

In the CONN toolbox, a total of 164 ROIs (6-mm spheres) are defined as seeds, where 132 ROIs are from the cortical and subcortical areas of the brain software library (FSL) Harvard-Oxford atlas, as well as cerebellar areas of the automated anatomical labeling (AAL) atlas, and 32 ROIs are from the atlases of 8 functional networks (default mode network, sensorimotor network, visual networks, salience networks, dorsal attention networks, fronto-parietal networks, language networks, cerebellar networks) [24]. From these 164 ROIs, we selected 133 areas as seeds in this study for the seed-to-voxel analysis. These ROIs correspond to brain areas thought to be involved in language processing and speech production. The names of the selected ROIs and the coordinates of the centers of the spheres are given in Table 2.

**Table 2.** Information of the selected seed ROIs from CONN toolbox.

No.	Seed's Name	MNI Coordinates
1.	FP r (Frontal Pole Right)	(26, 52, 8)
2.	FP l (Frontal Pole Left)	(-25, 53, 8)
3.	IC r (Insular Cortex Right)	(37, 3, 0)
4.	IC l (Insular Cortex Left)	(-36, 1, 0)
5.	SFG r (Superior Frontal Gyrus Right)	(15, 18, 57)
6.	SFG l (Superior Frontal Gyrus Left)	(-14, 19, 56)
7.	MidFG r (Middle Frontal Gyrus Right)	(39, 19, 43)
8.	MidFG l (Middle Frontal Gyrus Left)	(-38, 18, 42)
9.	IFG tri r (Inferior Frontal Gyrus, pars triangularis Right)	(52, 28, 8)
10.	IFG tri l (Inferior Frontal Gyrus, pars triangularis Left)	(-50, 28, 9)
11.	IFG oper r (Inferior Frontal Gyrus, pars opercularis Right)	(52, 15, 16)
12.	IFG oper l (Inferior Frontal Gyrus, pars opercularis Left)	(-51, 15, 15)
13.	PreCG r (Precentral Gyrus Right)	(35, -11, 50)
14.	PreCG l (Precentral Gyrus Left)	(-34, -12, 49)
15.	TP r (Temporal Pole Right)	(41, 13, -30)
16.	TP l (Temporal Pole Left)	(-40, 11, -30)
17.	aSTG r (Superior Temporal Gyrus, anterior division Right)	(58, -1, -10)
18.	aSTG l (Superior Temporal Gyrus, anterior division Left)	(-56, -4, -8)
19.	pSTG r (Superior Temporal Gyrus, posterior division Right)	(61, -24, 2)
20.	pSTG l (Superior Temporal Gyrus, posterior division Left)	(-62, -29, 4)
21.	aMTG r (Middle Temporal Gyrus, anterior division Right)	(58, -2, -25)
22.	aMTG l (Middle Temporal Gyrus, anterior division Left)	(-57, -4, -22)
23.	pMTG r (Middle Temporal Gyrus, posterior division Right)	(61, -23, -12)
24.	pMTG l (Middle Temporal Gyrus, posterior division Left)	(-61, -27, -11)
25.	toMTG r (Middle Temporal Gyrus, temporooccipital part Right)	(58, -49, 2)
26.	toMTG l (Middle Temporal Gyrus, temporooccipital part Left)	(-58, -53, 1)
27.	aITG r (Inferior Temporal Gyrus, anterior division Right)	(46, -2, -41)
28.	aITG l (Inferior Temporal Gyrus, anterior division Left)	(-48, -5, -39)
29.	pITG r (Inferior Temporal Gyrus, posterior division Right)	(53, -23, -28)
30.	pITG l (Inferior Temporal Gyrus, posterior division Left)	(-53, -28, -26)
31.	toITG r (Inferior Temporal Gyrus, temporooccipital part Right)	(54, -50, -17)
32.	toITG l (Inferior Temporal Gyrus, temporooccipital part Left)	(-52, -53, -17)
33.	PostCG r (Postcentral Gyrus Right)	(38, -26, 53)
34.	PostCG l (Postcentral Gyrus Left)	(-38, -28, 52)
35.	SPL r (Superior Parietal Lobule Right)	(29, -48, 59)
36.	SPL l (Superior Parietal Lobule Left)	(-29, -49, 57)
37.	aSMG r (Supramarginal Gyrus, anterior division Right)	(58, -27, 38)
38.	aSMG l (Supramarginal Gyrus, anterior division Left)	(-57, -33, 37)
39.	pSMG r (Supramarginal Gyrus, posterior division Right)	(55, -40, 34)
40.	pSMG l (Supramarginal Gyrus, posterior division Left)	(-55, -46, 33)
41.	AG r (Angular Gyrus Right)	(52, -52, 32)
42.	AG l (Angular Gyrus Left)	(-50, -56, 30)
43.	ICC r (Intracalcarine Cortex Right)	(12, -74, 8)
44.	ICC l (Intracalcarine Cortex Left)	(-10, -75, 8)
45.	MedFC (Frontal Medial Cortex)	(0, 43, -19)

(continued on next page)

Table 2 (continued)

No.	Seed's Name	MNI Coordinates
46.	SMA r (Juxtapositional Lobule Cortex -formerly Supplementary Motor Cortex- Right)	(6, -3, 58)
47.	SMA l (Juxtapositional Lobule Cortex -formerly Supplementary Motor Cortex- Left)	(-5, -3, 56)
48.	SubCalC (Subcallosal Cortex)	(0, 21, -15)
49.	PaCiG r (Paracingulate Gyrus Right)	(7, 37, 23)
50.	PaCiG l (Paracingulate Gyrus Left)	(-6, 37, 21)
51.	AC (Cingulate Gyrus, anterior division)	(1, 18, 24)
52.	PC (Cingulate Gyrus, posterior division)	(1, -37, 30)
53.	Precuneous (Precuneous Cortex)	(1, -59, 38)
54.	FORb r (Frontal Orbital Cortex Right)	(29, 23, -16)
55.	FORl l (Frontal Orbital Cortex Left)	(-30, 24, -17)
56.	aPaHC r (Parahippocampal Gyrus, anterior division Right)	(22, -8, -30)
57.	aPaHC l (Parahippocampal Gyrus, anterior division Left)	(-22, -9, -30)
58.	pPaHC r (Parahippocampal Gyrus, posterior division Right)	(23, -31, -17)
59.	pPaHC l (Parahippocampal Gyrus, posterior division Left)	(-22, -32, -17)
60.	LG r (Lingual Gyrus Right)	(14, -63, -5)
61.	LG l (Lingual Gyrus Left)	(-12, -66, -5)
62.	aTFusC r (Temporal Fusiform Cortex, anterior division Right)	(31, -3, -42)
63.	aTFusC l (Temporal Fusiform Cortex, anterior division Left)	(-32, -4, -42)
64.	pTFusC r (Temporal Fusiform Cortex, posterior division Right)	(36, -24, -28)
65.	pTFusC l (Temporal Fusiform Cortex, posterior division Left)	(-36, -30, -25)
66.	FO r (Frontal Operculum Cortex Right)	(41, 19, 5)
67.	FO l (Frontal Operculum Cortex Left)	(-40, 18, 5)
68.	CO r (Central Opercular Cortex Right)	(49, -6, 11)
69.	CO l (Central Opercular Cortex Left)	(-48, -9, 12)
70.	PO r (Parietal Operculum Cortex Right)	(49, -28, 22)
71.	PO l (Parietal Operculum Cortex Left)	(-48, -32, 20)
72.	PP r (Planum Polare Right)	(48, -4, -7)
73.	PP l (Planum Polare Left)	(-47, -6, -7)
74.	HG r (Heschl's Gyrus Right)	(46, -17, 7)
75.	HG l (Heschl's Gyrus Left)	(-45, -20, 7)
76.	PT r (Planum Temporale Right)	(55, -25, 12)
77.	PT l (Planum Temporale Left)	(-53, -30, 11)
78.	SCC r (Supracalcarine Cortex Right)	(8, -74, 14)
79.	SCC l (Supracalcarine Cortex Left)	(-8, -73, 15)
80.	Thalamus r	(11, -18, 7)
81.	Thalamus l	(-10, -19, 6)
82.	Caudate r	(13, 10, 10)
83.	Caudate l	(-13, 9, 10)
84.	Putamen r	(25, 2, 0)
85.	Putamen l	(-25, 0, 0)
86.	Pallidum r	(20, -4, -1)
87.	Pallidum l	(-19, -5, -1)
88.	Hippocampus r	(26, -21, -14)
89.	Hippocampus l	(-25, -23, -14)
90.	Amygdala r	(23, -4, -18)
91.	Amygdala l	(-23, -5, -18)
92.	Accumbens r	(9, 12, -7)

Table 2 (continued)

No.	Seed's Name	MNI Coordinates
93.	Accumbens l	(-9, 11, -7)
94.	Brain-Stem	(0, -30, -35)
95.	Cereb1 l (Cerebellum Crus1 Left)	(-36, -66, -30)
96.	Cereb1 r (Cerebellum Crus1 Right)	(38, -67, -30)
97.	Cereb2 l (Cerebellum Crus2 Left)	(-29, -73, -38)
98.	Cereb2 r (Cerebellum Crus2 Right)	(32, -69, -40)
99.	Cereb3 l (Cerebellum 3 Left)	(-9, -37, -19)
100.	Cereb3 r (Cerebellum 3 Right)	(12, -35, -19)
101.	Cereb45 l (Cerebellum 4 5 Left)	(-14, -44, -17)
102.	Cereb45 r (Cerebellum 4 5 Right)	(16, -44, -19)
103.	Cereb6 l (Cerebellum 6 Left)	(-23, -58, -24)
104.	Cereb6 r (Cerebellum 6 Right)	(24, -58, -25)
105.	Cereb7 l (Cerebellum 7b Left)	(-32, -60, -45)
106.	Cereb7 r (Cerebellum 7b Right)	(33, -63, -48)
107.	Cereb8 l (Cerebellum 8 Left)	(-26, -55, -48)
108.	Cereb8 r (Cerebellum 8 Right)	(25, -56, -49)
109.	Cereb9 l (Cerebellum 9 Left)	(-11, -49, -46)
110.	Cereb9 r (Cerebellum 9 Right)	(9, -49, -46)
111.	Cereb10 l (Cerebellum 10 Left)	(-23, -34, -42)
112.	Cereb10 r (Cerebellum 10 Right)	(26, -34, -41)
113.	Ver12 (Vermis 1 2)	(1, -39, -20)
114.	Ver3 (Vermis 3)	(1, -40, -11)
115.	Ver45 (Vermis 4 5)	(1, -52, -7)
116.	Ver6 (Vermis 6)	(1, -66, -16)
117.	Ver7 (Vermis 7)	(1, -72, -25)
118.	Ver8 (Vermis 8)	(1, -64, -34)
119.	Ver9 (Vermis 9)	(1, -55, -35)
120.	Ver10 (Vermis 10)	(0, -46, -32)
121.	networks.SensoriMotor.Lateral (L)	(-55, -12, 29)
122.	networks.SensoriMotor.Lateral (R)	(56, -10, 29)
123.	networks.SensoriMotor.Superior	(0, -31, 67)
124.	networks.FrontoParietal.LPFC (L)	(-43, 33, 28)
125.	networks.FrontoParietal.PPC (L)	(-46, -58, 49)
126.	networks.FrontoParietal.LPFC (R)	(41, 38, 30)
127.	networks.FrontoParietal.PPC (R)	(52, -52, 45)
128.	networks.Language.IFG (L)	(-51, 26, 2)
129.	networks.Language.IFG (R)	(54, 28, 1)
130.	networks.Language.pSTG (L)	(-57, -47, 15)
131.	networks.Language.pSTG (R)	(59, -42, 13)
132.	networks.Cerebellar.Anterior	(0, -63, -30)
133.	networks.Cerebellar.Posterior	(0, -79, -32)

In addition to between group analysis, the relation between stuttering severity and connectivity pattern of the brain in the stuttering group was also investigated. Whole brain regression analysis using Pearson correlation coefficient was performed to determine the effect of stuttering severity in PDS group.

For statistical analysis of the results, we used random field theory (RFT [25]) to control the analysis-wise chance of false positives. Following the previous research [20] and considering that the analysis was performed for 133 seeds, cluster-level FDR (False Discovery Rate [26]) correction was adjusted to  $p < 3.76 \times 10^{-4}$  (i.e., dividing the 0.05  $\alpha$ -value by the 133 tested seeds based on the Bonferroni correction to address multiple comparisons). The results were considered significant at a voxel-wise threshold of level  $p < 0.001$  uncorrected and a cluster-level threshold of  $p < 3.76 \times 10^{-4}$  FDR corrected.

It is notable that we reported the results for each individual cluster as a measure of its location (the MNI coordinates of the peak voxel), cluster size, associated cluster-level p-values, the effect-size within the region (represented as  $r$ ), and peak-voxel statistical T value [27].

### 3. Results

#### 3.1. Resting state connectivity: group differences

Our results revealed abnormal RSFC in PDS as compared with the control group; decreased connectivity was observed between three left sided seeds and several brain areas as shown in Figure 1, while no seeds with significantly increased FC were found. Figure 1 depicts the location of the seed ROIs as well as a few slices of target subcortical regions with significant FC alterations in the PDS group. We also display our volume-based connectivity results on the surface for better visualization in Figure 2. It should be noted that we did not conduct the cortical and sub-cortical analysis separately; Figure 2 is only a surface-display of the volume-based connectivity results.

Compared to control participants, PDS exhibited decreased connectivity of: (i) left frontal pole (FPI) with right Rolandic operculum (Rolandic\_Oper), right precentral/postcentral gyrus, and right superior temporal gyrus (STGr); (ii) left middle frontal gyrus (MidFGl) with central opercular cortex, as well as right precentral/postcentral gyrus; (iii) left superior temporal gyrus, posterior division (pSTG1) with right limbic lobe, right fusiform, right hippocampal and right cerebellum, as well as

left middle occipital (MOccil) and left middle temporal gyrus (MTGI). Table 3 shows the detailed information.

As shown in Figure 2 (a), the RSFC between FPI and right sensory/motor areas (Rolandic\_Oper, precentral/postcentral gyrus; BA 13/43/6) as well as STGr (BA 22) was negative in both groups (control:  $r = -0.25$ , PDS:  $r = -0.01$ ). However, compared with controls, PDS subjects showed weaker negative connectivity ( $T(28) = -5.26$ ,  $r = -0.24$ ,  $p < 0.001$ ).

As shown in Figure 2 (b), the RSFC between MidFGl and right sensory/motor areas (precentral/postcentral gyrus; BA 3/1/4/6/2) was positive in the control group ( $r = 0.01$ ), while negative in the PDS group ( $r = -0.23$ ), which resulted in a significant difference between groups ( $T(28) = -5.79$ ,  $r = -0.24$ ,  $p < 0.001$ ).

Similarly, Figure 2 (c) shows altered connectivity in the PDS vs. control subjects between pSTG1 and two clusters: (i) right limbic lobe and hippocampus (BA 37/35/36/20), with positive FC in the control group ( $r = 0.12$ ) and negative FC in the PDS group ( $r = -0.09$ ), and significant difference in FC between the two groups ( $T(28) = -7.26$ ,  $r = -0.21$ ,  $p < 0.001$ ); (ii) MOccipl and MTGI (BA 19/18/37), with positive FC in the control group ( $r = 0.15$ ) and negative FC in the PDS group ( $r = -0.08$ ), and significant difference in FC between the two groups ( $T(28) = -6.37$ ,  $r = -0.23$ ,  $p < 0.001$ ).

#### 3.2. Resting state connectivity: stuttering symptom correlations

Apart from between-group comparison, the regression analysis has been performed utilizing the stuttering severity scores as the regressor to investigate if there is a correlation between RSFCs and the stuttering severity in the PDS group. These results are presented in Figures 3 and 4 and details are given in Table 4.

The results revealed that the stuttering severity was positively correlated with RSFCs between: (a, b) right cerebellum and left occipital lobe; (c) MidFGl and left occipital lobe; and (d) left para-hippocampal (pPaHCl) and left inferior/superior parietal gyrus (IPGl/SPGl). In addition, we observed several patterns of negative correlation between: (e) right middle temporal gyrus, anterior division (aMTGr), and IFGl as well as STGI; (f) right fronto-orbital (FORbr) and MTGr as well as right inferior temporal gyrus (ITGr); and (g) left caudate and middle frontal left (MidFl).

To inspect whether these patterns of correlations were observed due to extremely low or high connectivity in the PDS individuals as a whole,

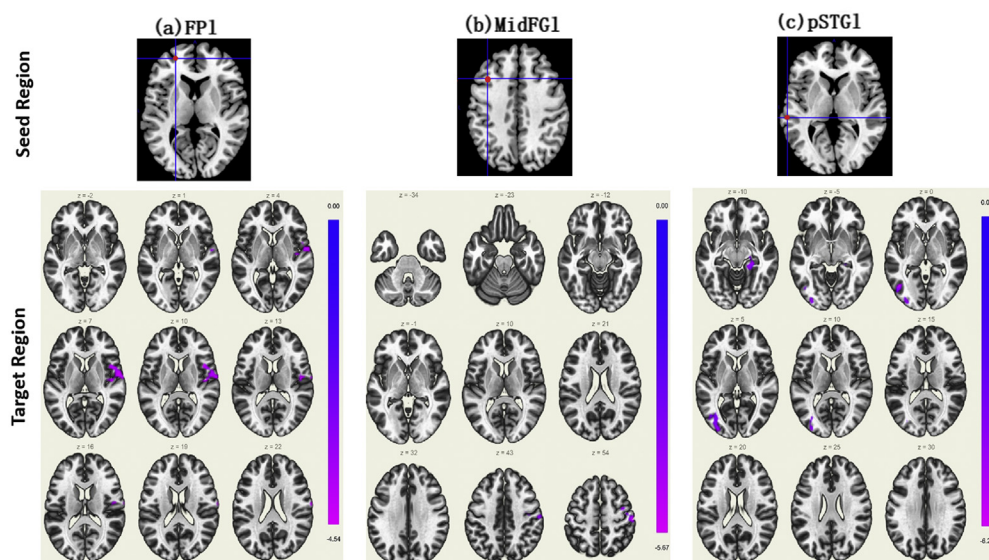


**Figure 1.** RSFC alternations in PDS subjects vs. control group. Thresholds are Voxelwise  $p < 0.001$  uncorrected, cluster  $p < 3.76 \times 10^{-4}$  FDR corrected. The first row shows the location of the seed region centered at cross line; the second row depicts the slice view of FC map. (a) FC maps generated based on the FPI seed. (b) FC maps generated based on the MidFGl seed. (c) FC maps generated based on the pSTG1 seed.

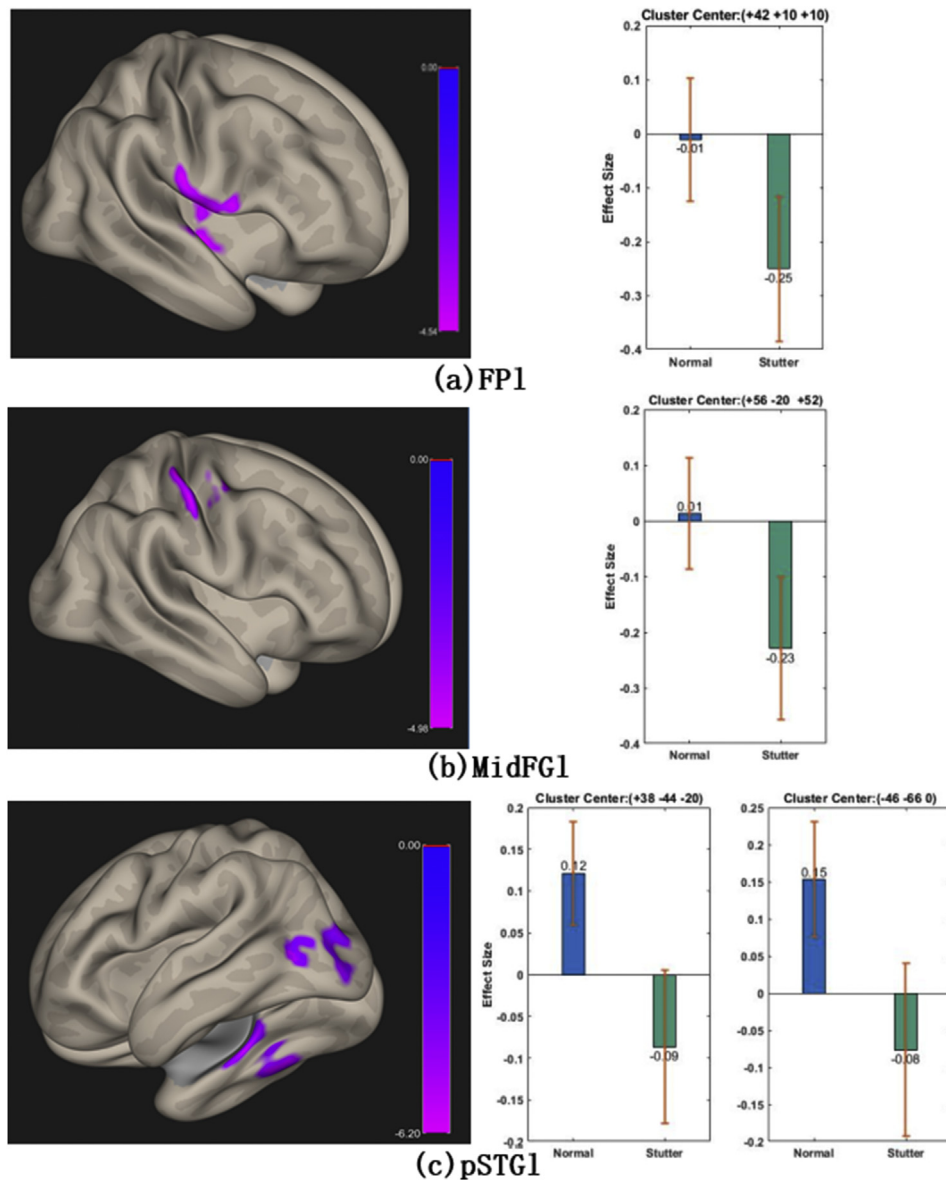


**Figure 2.** RSFC alternations in PDS subjects vs. control group. Thresholds are Voxelwise  $p < 0.001$  uncorrected, cluster  $p < 3.76 \times 10^{-4}$  FDR corrected. Left column shows the connectivity map; right column depicts pair-wise effect size showing the group differences for correlations between the seeds and significant clusters. (a) FC maps generated based on the FPI seed. (b) FC maps generated based on the MidFGI seed. (c) FC maps generated based on the pSTGI seed.

the connectivity measures for these connections between PDS and the control groups have been further compared. For this purpose, the FC between the selected seeds, tabulated in Table 4, and the observed target regions in this table have been analyzed for each group individually.

Although the RSFC between Cereb1r and left occipital lobe (Figure 3a and Figure 4a) was positively correlated with severity of stuttering ( $R = 0.91$ ,  $R$  is the effect size equal to Pearson correlation), but their FC was insignificant in both groups (PDS:  $r = -0.00$ ,  $p = 0.94$ ; controls:  $r = -0.30$ ,  $p = 0.5$ ; PDS vs. control:  $r = 0.03$ ,  $p = 0.65$ ).

Similarly, RSFC between Cereb7r and left occipital lobe as shown in Figure 3b and Figure 4b was positively correlated with severity of stuttering ( $R = 0.86$ ), but their FC was insignificant in both groups (PDS:  $r = 0.05$ ,  $p = 0.32$ ; controls:  $r = 0.02$ ,  $p = 0.60$ ; PDS vs. control:  $r = 0.04$ ,  $p = 0.54$ ).

As shown in Figure 3c and Figure 4c, stuttering severity was positively correlated with RSFC between MidFGI and again left occipital lobe ( $R = 0.89$ ), however their FC was insignificant in both groups (PDS:  $r = -0.06$ ,  $p = 0.24$ ; controls:  $r = -0.03$ ,  $p = 0.41$ ; PDS vs. control:  $r = -0.02$ ,  $p = 0.71$ ).

The RSFC between aMTGr and IFGI/STGI as shown in Figure 3d and Figure 4d was negatively correlated with stuttering severity, however no significant FC was observed between them at each group (PDS:  $r = -0.00$ ,  $p = 0.96$ ; controls:  $r = 0.02$ ,  $p = 0.74$ ; PDS vs. control:  $r = -0.02$ ,  $p = 0.80$ ).

Again, RSFC between FORbr and MTGr/ITGr was positively correlated with stuttering severity as shown depicted in Figure 3e and Figure 4e ( $R = -0.89$ ), but there is no significant FC between them at each group (PDS:  $r = 0.04$ ,  $p = 0.45$ ; controls:  $r = 0.17$ ,  $p = 0.005$ ; PDS vs. control:  $r = -0.12$ ,  $p = 0.11$ ).

The RSFC between pPaHCl and IPGI/SPGI as shown in Figure 3f and Figure 4f was positively correlated with stuttering severity ( $R = 0.90$ ), however no significant FC was observed between them at each group (PDS:  $r = -0.04$ ,  $p = 0.33$ ; controls:  $r = -0.07$ ,  $p = 0.17$ ; PDS vs. control:  $r = 0.02$ ,  $p = 0.73$ ).

Finally, as depicted in Figure 3g and Figure 4g, stuttering severity was negatively correlated with RSFC between left caudate and left middle frontal regions ( $R = -0.86$ ), however their FC was insignificant in both

**Table 3.** Functional connectivity alterations in PDS subjects.

Seed ROI	Source Centre (x, y, z)	Target Region	Target Centre (x, y, z)	BA	I/D	Effect Size	T-value	p-value		Cluster size (number of voxels)
								Voxel-level	Cluster-level (FDR)	
atlas.FP l (Frontal Pole Left)	(−25, 53, 8)	Rolandic_Oper_R (aal), Right Precentral Gyrus, Right Superior Temporal Gyrus, Insula_R (aal), Right Postcentral Gyrus	(42, 10, 10)	13, 22, 43, 6	D	−0.24	−5.26	$0.1 \times 10^{-5}$	$1.5 \times 10^{-5}$	667
atlas.MidFG l (Middle Frontal Gyrus Left)	(−38, 18, 42)	Central Opercular Cortex, Postcentral_R (aal), Precentral_R (aal)	(56, −20, 52)	3, 1, 4, 6, 2	D	−0.24	−5.79	$0.4 \times 10^{-5}$	$1.16 \times 10^{-4}$	554
atlas.pSTG l (Superior Temporal Gyrus, posterior division Left)	(−62, −29, 4)	Limbic Lobe_R, Fusiform_R (aal), ParaHippocampal_R (aal), R Cerebellum Anterior Lobe, Hippocampus_R (aal)	(38, −44, −20)	37, 35, 36, 20	D	−0.21	−7.26	$< 0.1 \times 10^{-5}$	$0.2 \times 10^{-5}$	784
		Occipital_Mid_L (aal), Temporal_Mid_L (aal)	(−46, −66, 0)	19, 18, 37	D	−0.23	−6.37	$0.1 \times 10^{-5}$	$1.2 \times 10^{-5}$	608

The center of the maximum pixel values at target clusters are expressed based on the MNI coordinates. Voxel-wise  $p < 0.001$  uncorrected, cluster  $p < 3.76 \times 10^{-4}$  FDR corrected,  $|T(28)| \geq 3.41$ .

Abbreviations: L = left; R = right; BA = Brodmann's area; I/D = Increased or Decreased connectivity.

groups (PDS:  $r = 0.06$ ,  $p = 0.16$ ; controls:  $r = 0.03$ ,  $p = 0.43$ ; PDS vs. control:  $r = 0.03$ ,  $p = 0.63$ ).

### 3.3. Effect of spatial smoothing on connectivity patterns

Spatial smoothing is a common preprocessing step usually applied to reduce the amount of noise in fMRI data, increase the signal-to-noise ratio (SNR), as well as compensate for inaccuracies in spatial registration and decrease the inter-subject variability. However, smoothing may induce the undesired signal contamination in brain areas that are close together [28]. As shown in the previous results (Figures 2 and 3), some target clusters may span multiple brain regions across neighboring gyri. This is likely due to the large smoothing kernel where the smoothing was not restricted within each subcortical structure or restricted to grey matter.

Here, to check how spatial smoothing affects the observed differences in brain network connectivity between subject groups, we re-analyzed the data by reducing the smoothing kernel size to 6 mm. Figure 5 shows the results. Decreased connectivity between pSTG1 and left occipital pole in the PDS group is the only result in this analysis. As expected, smaller smoothing kernel size, decreased the connection strength between voxels, leading to detection of smaller clusters of voxels connected with the seed. However, some of our previous results (section 3.1) are no more significant.

In practice, for most purposes, it is recommended to select a kernel FWHM size as 2–3 times the functional voxel size, where the larger filters may be useful if the signal to noise ratio is particularly bad, and the activation expected to cover a large area, whilst a narrower filter can be used if the SNR is good enough [29].

## 4. Discussion

### 4.1. Deficits of RSFCs in PDS group

The present study investigated RSFC differences between PDS and healthy control participants. Consistent with a previous rsfMRI study on stuttering individuals [2], we found that PDS exhibited decreased RSFCs of the particular regions in the left frontal gyrus relative to control subjects. Our results revealed that several left-sided frontal areas, including FPl and MidFGl, had decreased connectivity with the right precentral/postcentral gyrus.

Left frontal regions are well studied as the main cortical regions mediating lexical access and semantic processing steps in language production [30, 31]. A PET study on the comparison of patients with DS and

normal controls showed decreased metabolism in frontal areas such as IFG and FP and Wernicke area in DS patients [32]. Regarding the role of FP in language processing, previous studies suggest the involvement of bilateral FP in narrative processing [33].

MidFG plays a key role in language processing networks. This region is involved in expressive language processing such as semantics, verbal fluency, grammar and syntax, and phonological working memory performances [34]. Since phonological working memory function is essential for the maintenance and manipulation of verbal information such as serial ordering of linguistic information, the relation between phonological working memory and language production is undeniable [35, 36].

The involvement of MidFGl in language processing has been also reported by several neuroimaging studies [37, 38]. Based on previous task-evoked fMRI findings, MidFGl is usually involved across different languages in word reading [39, 40, 41].

The right Rolandic operculum, in the premotor cortex, has been involved in processing sentence intonation in healthy individuals [42] and right STG is involved in processing language prosody in intonation processing. This could explain the altered FC between the FPl/MidFGl and right Rolandic and STG in stuttering subjects. That is, in the PDS group, the altered connectivity between left frontal and right STG and Rolandic operculum could lead a deficit in integrating the processes of language fluency, intonation, and prosody in the process of language production as well as controlling the actual speech movements.

Moreover, our finding indicated the abnormal FC between pSTG1 and several brain regions including right limbic lobe, right fusiform, right hippocampal and right cerebellum, as well as MOccil and MTG1. Altered activation of pSTG1 in stuttering related researches has been reported frequently [15, 43, 44]. The pSTG1 is involved in phonological lexical processing in both comprehension and production of language [45, 46]. Although language perception appears to involve pSTG bilaterally, particularly with respect to phonemic information [45, 47].

Since the emotional language was processed through the limbic system, the abnormal decoupling between the pSTG1 and right limbic system (hippocampal/para-hippocampal) in stuttering subjects may result in difficulties in the expression of emotion for speech production. Indeed, the role of anxiety which is regulated by the limbic system with stuttering disorder has been previously studied by neuroimaging techniques [48]. Beyond the emotional aspect, the altered FC between the right cerebellum and pSTG1 has been evidenced in stuttering people, supporting the view that cerebellum has a high level of motor/cognitive function by coupling with primary language areas such as Wernicke area (a part of STG1). Indeed, the cerebellum plays a crucial role in a wide variety of complex behaviors like speech. There are evidences for the presence of

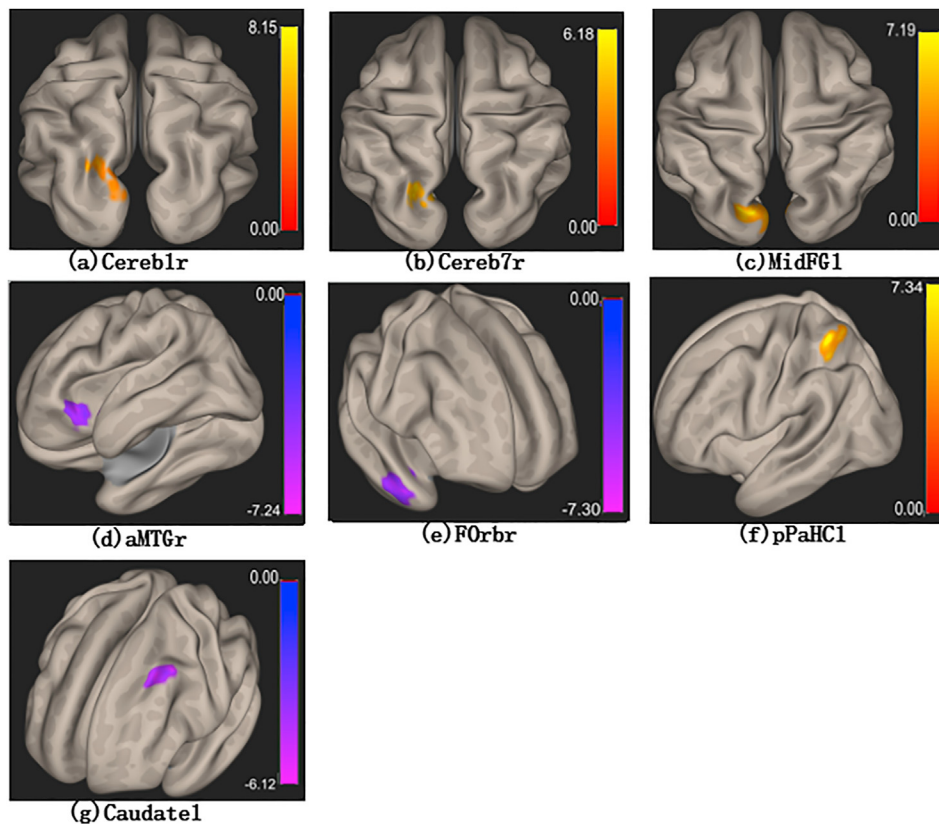


**Figure 3.** Correlation between RSFCs within brain regions and severity of stuttering. Thresholds are Voxelwise  $p < 0.001$  uncorrected, cluster  $p < 3.76 \times 10^{-4}$  FDR corrected. (a)–(b) Correlation maps generated based on Cerebellum right seeds (Cereb1r, Cereb7r). (c) Correlation maps generated based on the MidFGI seed. (d) Correlation maps generated based on the aMTGr seed. (e) Correlation maps generated based on the FOrrbr seed. (f) Correlation maps generated based on the pPaHC1 seed, (g) Correlation maps generated based on the left Caudate (Caudatel) seed.

communication circuits between the cerebellum and a wide range of cortical and subcortical areas, supporting its role in both motor planning and motor coordination in speech production and language perception [49], in verbal working memory, in phonological and semantic verbal fluency, in syntax processing, and in the dynamics of language production [50]. A meta-analysis of neuroimaging researches investigating the cerebellar involvement in motor and cognitive functions provided the support that anterior portions of the cerebellum are part of motor networks, whereas the majority of the posterior regions are associated with cognitive functions [50, 51].

furthermore, activation in MTG and STG has been reported in response to listening to sentences, as well as speech vs. non-speech stimuli in healthy individuals [52]. These observations emphasize the involvement of these two regions in phonemic and phonological language perception. This can explain a part of the results observed in the present work; decreased FC between the pSTG1 and MTG1. We may conclude that one affected component in language production in adult individuals who stutter could be the process of phonemic and phonological perception.

#### 4.2. Stuttering symptom correlations

In addition, the correlation analysis between FC and severity of stuttering revealed the compensatory connectivity pattern in less symptomatic PDS. We found that stutterers with the least severe symptoms had greater functional connectivity between left caudate and MidFG1. The correlation of caudate activity with stuttering severity has been documented in previous studies [53]. Indeed, caudate not only has been involved in the smooth organization of motor actions and speech-related movements, but also implicated in learning, memory, emotion, and language processing [54].

We also found that stutterers with less severe symptoms had greater FC between right MTG and several regions in the left cerebrum including IFG, as well as STG. These results imply that although the connectivity of

STG1 with MTG1 was impaired in the PDS group, a compensatory mechanism induced a greater FC with MTGr. This is in line with results of Braun et al. [55] who studied cerebral activity patterns in individuals who stutter. The authors reported that there are compensatory processes mediated by right hemispheric cerebral regions to attenuate stuttering symptoms.

In a similar way, the connectivity between FOrrbr and MTGr was also negatively correlated with stuttering severity. This finding may also be explained by the involvement of MTGr and frontal regions in successful compensatory mechanisms developed in more fluent stutterers.

An increased connectivity between the right cerebellar and left occipital regions in more severe PDS cases was also observed. This increased connectivity could be potentially related to increased demand on high order cognitive processes in language production, i.e., phonological-semantic (right cerebellum) and lexical code (lingual gyrus of occipital lobe) connections [56].

Interestingly, we observed an increased FC between left frontal and occipital regions in individuals with more stuttering severity. There is compelling evidence on the presence of "dorsal and ventral streams" which may process the phonological and semantic aspects of language, respectively [57]. The ventral pathway involves a fronto-occipital structural connection, which subserves semantic processing. The observed connectivity pattern in the present study can be explained as a compensatory mechanism in more severe cases. That is, while in more severe cases the connectivities related to phonemic and phonological processing are weaker, they demonstrate stronger functional connectivity in regions which mediate semantic processing. However, because this compensatory mechanism is not efficient, their language production performance does not improve.

There is very limited data regarding the positive correlation of stuttering severity with FC between pPaHC1 and IPG1/SPG1 which we observed in our results. Our results may support the role of parietal cortex in processing somatosensory feedback during speech production [58]. This result may suggest the contribution of these regions in the control of

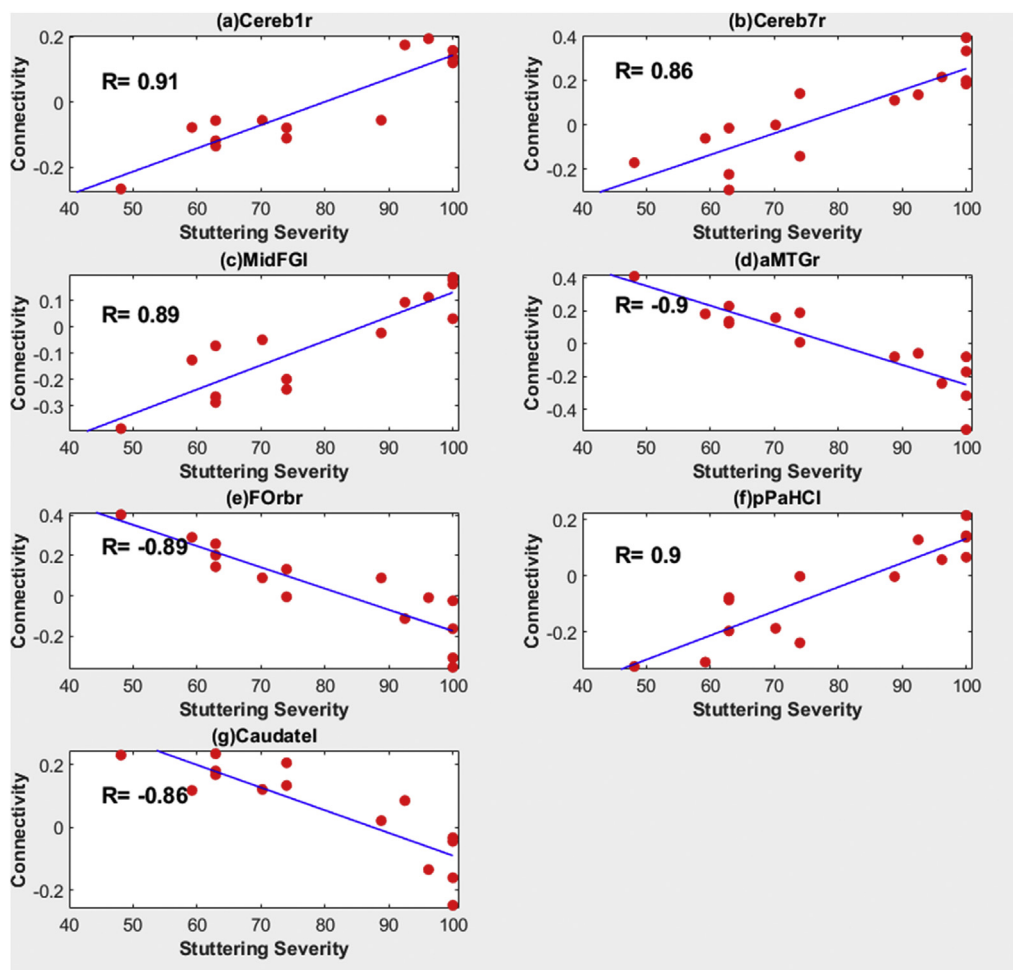


**Figure 4.** Correlation plots between RSFCs within brain regions and severity of stuttering. R = Pearson correlation value. The names of the seed regions are written on the top of the plots. (a) Correlation between stuttering severity and RSFC of source seed Cereb1r and target region indicated in Figure 3(a). (b) Correlation between stuttering severity and RSFC of source seed Cereb7r and target region indicated in Figure 3(b). (c) Correlation between stuttering severity and RSFC of source seed MidFGl and target region indicated in Figure 3(c). (d) Correlation between stuttering severity and RSFC of source seed aMTGr and target region indicated in Figure 3(d). (e) Correlation between stuttering severity and RSFC of source seed FORbr and target region indicated in Figure 3(e). (f) Correlation between stuttering severity and RSFC of source seed pPaHCl and target region indicated in Figure 3(f). (g) Correlation between stuttering severity and RSFC of source seed Caudatel and target region indicated in Figure 3(g).

**Table 4.** Correlation between RSFCs within brain regions and severity of stuttering.

Seed ROI	Source Centre (x, y, z)	Target Region	Target Centre (x, y, z)	BA	Cor.	Effect Size (Z)	T-value	p-value		Cluster size (number of voxels)
								Voxel-level	Cluster-level (FDR)	
atlas.Cereb1 r (Cerebellum Crus1 Right)	(38, -67, -30)	Occipital_Sup_L (aal), Left Parietal Lobe, Cuneus_L (aal)	(-22, 19, -74, 36)	19, 7, 18	+	0.91 (0.74)	8.14	$0.3 \times 10^{-5}$	$7.3 \times 10^{-5}$	370
atlas.Cereb7 r (Cerebellum 7b Right)	(33, -63, -48)	Occipital_Sup_L (aal), Left Precuneus, Sub-Gyral,	(-20, 7, 19, -76, 30)	7, 19	+	0.86 (0.71)	6.18	$2.2 \times 10^{-5}$	$3.53 \times 10^{-4}$	338
atlas.MidFGl (Middle Frontal Gyrus Left)	(-38, 18, 42)	Cuneus_L (aal), Occipital_Sup_L (aal), Left Precuneus,	(-8, 19, -88, 40)	19, 18, 31	+	0.89 (0.72)	7.19	$0.0 \times 10^{-5}$	$0.0 \times 10^{-5}$	860
atlas.aMTG r (Middle Temporal Gyrus, anterior division Right)	(58, -2, -25)	Left Inferior Frontal Gyrus, Frontal_Inf_Orb_L (aal), Left Superior Temporal Gyrus, Temporal_Pole_Sup_L (aal)	(-54, 47, 16, -12)	47, 38	-	-0.90 (-0.73)	-7.27	$0.2 \times 10^{-5}$	$4.7 \times 10^{-5}$	453
atlas.FORb r (Frontal Orbital Cortex Right)	(29, 23, -16)	Temporal_Mid_R (aal), Temporal_Pole_Mid_R (aal), Temporal_Inf_R (aal)	(48, 6, -26)	21	-	-0.89 (-0.73)	-7.30	$0.4 \times 10^{-5}$	$6.5 \times 10^{-5}$	435
atlas.pPaHCl (Parahippocampal Gyrus, posterior division Left)	(-22, -32, -17)	Parietal_Inf_L (aal), Parietal_Sup_L (aal)	(-38, -52, 62)	40, 7	+	0.90 (0.73)	7.34	$0.2 \times 10^{-5}$	$2.4 \times 10^{-5}$	370
atlas.Caudate l	(-13, 9, 10)	Frontal_Mid_L (aal)	(-32, 14, 46)	6, 8	-	-0.86 (-0.71)	-6.12	$2.1 \times 10^{-5}$	$3.73 \times 10^{-4}$	323

The center of the maximum pixel values at target clusters are expressed based on the MNI coordinates. Voxel-wise  $p < 0.001$  uncorrected, cluster  $p < 3.76 \times 10^{-4}$  FDR corrected,  $|T(13)| \geq 3.85$ .

Abbreviations: L = left; R = right; BA = Brodmann's area, Cor = Correlation sign, Z = Fisher transformed correlation.

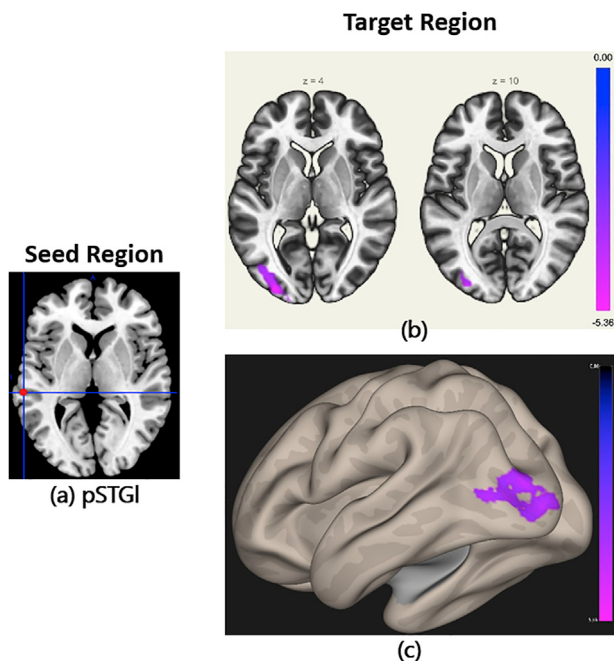


**Figure 5.** RSFC alternations in PDS subjects vs. control group (smoothing kernel size = 6mm). Thresholds are Voxelwise  $p < 0.001$  uncorrected, cluster  $p < 3.76 \times 10^{-4}$  FDR corrected. The left column shows the location of seed ROI; the right column depicts the FC map. (a) pSTGI seed. (b) Slice view. (c) Surface view.

the perturbation in oropharyngeal movements in severe cases of stuttering.

### 4.3. Comparison to previous works

In the end, for ease of comparing the results of this study with previous similar works, we provided the important details of rsfMRI researches on stuttering (both adults and children) including methodology, number of subjects, and main finding in Table 5.

Briefly, part of our results extends previous findings in the literature, while our results supported the contribution of pSTGI in stuttering disorder fall in line with those from previous studies [2]. However, our other interesting findings related to altered FC between the FPI/MidFGI and motor areas have less support in the literature.

## 5. Conclusion

This study investigated the functional connectivity in Persian-speaking adults with PDS disorder compared to control group. Our findings reflect the abnormalities which affect language planning and motor execution for fluent speaking, as well as the compensatory mechanisms of the brain to overcome or alleviate the stuttering symptoms.

In this study, we showed that the altered functional connectivity between the FPI/MidFGI and motor areas, as well as between STGI and several brain regions including the right limbic lobe (hippocampal/parahippocampal) and right cerebellum in stuttering subjects are the neurological underlying impairments regarding speech disfluency.

Additionally, stronger functional connections between MidFGI and left caudate, as well as between MTGr and language areas in the left cerebrum (Broca's and Wernicke's area), with decreased stuttering symptom severity in PDS, suggest that impaired function of these cortical/subcortical regions may enable the most successful compensation for stuttering symptoms.

**Table 5.** rsfMRI studies of stuttering.

Study	Method	Statistical analysis	Sample (mean age)	Main finding
[10]	ICA based RSFC comparison before and after speech therapy.	$P < 0.05$ , corrected by Monte Carlo simulation, individual voxel $p < 0.001$ , cluster volume $> 327 \text{ mm}^3$ .	13 controls (24) 15 PDS (24)	RSFC was decreased in the cerebellum after therapy to the level of fluent controls.
[2]	ROI-based RSFC	$P < 0.05$ , corrected by family-wise error (FWE) and cluster size $< 35$ voxels.	46 controls (25.2) 44 PDS (25.4)	Reduced FC between the posterior language reception area and anterior brain regions related to initiation of speech motor, but increased FC within anterior/posterior speech associated regions in the PDS group
[5]	Seed-voxel based RSFC	voxel-wise $p < 0.005$ uncorrected with cluster size $> 64$ voxels corresponding to $p < 0.03$ whole brain corrected using Monte Carlo simulation.	18 control (24.7) 16 PDS (26.3)	Decreased connectivity between the basal ganglia and right SMA, as well as bilateral STG, but increased connectivity between the cerebellum and right IFG in the PDS group
[15]	Seed-voxel based RSFC	voxel-based $p < 0.005$ was corrected to be an equivalent whole-brain $p < 0.032$	29 controls (6.4) 27 stuttering children (6.4)	Reduced FC in networks that support self-initiated timing of speech movement, and integration of auditory feedback to speech motor control processes in stuttering children
[53]	ROI-based RSFC	uncorrected threshold of $p < 0.033$	19 control (24.5) 20 PDS (25.5)	Increased FC between cerebellum and thalamus, but decreased FC within the perisylvian auditory, motor, and speech planning regions in the PDS group
Our study	Seed-voxel based RSFC	Voxel-wise $p < 0.001$ uncorrected, cluster $p < 3.76 \times 10^{-4}$ FDR corrected	15 controls (25.7) 15 PDS (27.9)	Decreased FC between MidFGI and right motor areas, as well as between STGI and several brain regions including the right limbic lobe and right cerebellum in the PDS subjects

## 6. Limitations of the study

It should be noted that for fMRI-based RSFC analysis, the scanner's sound (audio noise) may lead to changes in brain activation, especially for stuttering patients. Although the participants were interviewed after scanning to ensure that there were no changes in their psychological

states, previous work demonstrated problematic effects of scanner's sound in the study of the auditory pathway and language [59]. Therefore, in such fMRI studies, it is recommended to use MRI sequences that are as silent as possible (to reduce the participant's anxiety or stress and diminish anxiety-related brain activation) and also minimize the scanning time as much as possible.

Another limitation of the present study is the number of participants. Although several fMRI studies with relatively similar samples have been widely published in the literature, it is notable that the small sample size may lead to higher variability in the data and in turn may cause limited reliability.

In addition, an analytical limitation of this study is that the FC analysis has been performed on volumetric data and displayed on the surface of the brain, in which the volumetric smoothing may induce the signal contamination in brain areas that are close together in the folded cortex. Theoretically, the surface-based smoothing on the unfolded cortex should enhance the ability to separate the signals between brain regions that are close together in the folded cortex but are more distant in the unfolded cortex [28]. Therefore, the surface-based analysis of the data may overcome this issue and improve the validity of activity and connectivity results.

## Declarations

### Author contribution statement

Seyedehsamaneh Shojaeilangari: Conceived and designed the experiments; Performed the experiments; Analyzed and interpreted the data; Contributed reagents, materials, analysis tools or data; Wrote the paper.

Narges Radman: Conceived and designed the experiments; Analyzed and interpreted the data; Wrote the paper.

Mohammad Ehsan Taghizadeh, Hamid Soltanian-Zadeh: Conceived and designed the experiments; Wrote the paper.

### Funding statement

This work was supported by the Iran's National Elites Foundation and the Institute for Research in Fundamental Sciences (IPM).

### Data availability statement

Part of their longitudinal study for stuttering disorder, we are working on this data for future publication as well.

### Declaration of interests statement

The authors declare no conflict of interest.

### Additional information

No additional information is available for this paper.

## Acknowledgements

The authors thank the National Brain Mapping Laboratory (NBML), Tehran, Iran, for MRI data acquisition. We also thank the Mind Enabling Centre as well as Dr. Hossein Dehghani Tafti and Mr. Erfan Vajdi for their help in recruiting potential participants and thank all the participants who took part in this study.

## References

- [1] J.V. Ashurst, M.N. Wason, Developmental and persistent developmental stuttering: an overview for primary care physicians, *J. Am. Osteopath. Assoc.* 111 (10) (2011) 576–580.

- [2] Y. Xuan, et al., Resting-state brain activity in adult males who stutter, *PLoS One* 7 (1) (2012).
- [3] T. Loucks, S. Jo, A. Leen, H. Sharma, N.G. Ambrose, Functional brain activation differences in stuttering identified with a rapid fMRI sequence, *J. Fluency Disord.* 36 (4) (2011) 302–307.
- [4] S.-E. Chang, Research updates in neuroimaging studies of children who stutter, *Semin. Speech Lang.* 35 (2) (2014) 67–79.
- [5] Y. Yang, F. Jia, W.T. Siok, L.H. Tan, Altered functional connectivity in persistent developmental stuttering, *Nat. Publ. Gr.* 6 (2016) 1–8.
- [6] T. Halag-Milo, et al., Beyond production: brain responses during speech perception in adults who stutter, *NeuroImage Clin.* 11 (2016) 328–338.
- [7] H.J. Biswal, B. F.Z. Yetkin, V.M. Haughton, Functional connectivity in the motor cortex of resting human brain using echo-planar MRI, *Magn. Reson. Med.* 34 (4) (1995) 537–541.
- [8] M.E.R. Michael D. Fox, Abraham Z. Snyder, Justin L. Vincent, Maurizio Corbetta, David C. Van Essen, The human brain is intrinsically organized into dynamic, anticorrelated functional networks, *Proc. Natl. Acad. Sci. Unit. States Am.* 102 (27) (2005) 9673–9678.
- [9] M.D. Fox, M. Greicius, Clinical applications of resting state functional connectivity, *Front. Syst. Neurosci.* 4 (June) (2010) 19.
- [10] C. Lu, et al., Neural anomaly and reorganization in speakers who stutter: a short-term intervention study, *Neurology* 79 (7) (2012) 625–632.
- [11] C. Lu, et al., Relationship between speech production and perception in people who stutter, *Front. Hum. Neurosci.* 10 (May) (2016) 1–11.
- [12] J. Desai, et al., "Reduced perfusion in Broca's area in developmental stuttering, *Hum. Brain Mapp.* 38 (4) (2017) 1865–1874.
- [13] A.C. Etchell, O. Civier, K.J. Ballard, P.F. Sowman, A systematic literature review of neuroimaging research on developmental stuttering between 1995 and 2016, *J. Fluency Disord.* 55 (2018) 6–45.
- [14] S.-E. Chang, Using brain imaging to unravel the mysteries of stuttering, *Cerebrum* 2011 (August) (2011) 12.
- [15] S.E. Chang, D.C. Zhu, Neural network connectivity differences in children who stutter, *Brain* 136 (12) (2013) 3709–3726.
- [16] M. Bakhtiar, S. Seifpanahi, H. Ansari, M. Ghanadzade, A. Packman, Investigation of the reliability of the SSI-3 for preschool Persian-speaking children who stutter, *J. Fluency Disord.* 35 (2) (2010) 87–91.
- [17] Mehdi Bakhtiar, H. Ansari, A. Packman, Translating the stuttering severity instrument (SSI-3) into Persian: response to Karimi, Nilipour, Shafiei and Howell, *J. Fluency Disord.* 36 (3) (2011).
- [18] J.C. Wakefield, DSM-5: an overview of changes and controversies, *Clin. Soc. Work. J.* 41 (2) (2013) 139–154.
- [19] R. Oldfield, The assessment and analysis of handedness: the Edinburgh inventory, *Neuropsychologia* 9 (1) (1971) 97–113.
- [20] M.J. Torres-Prioris, et al., Neurocognitive signatures of phonemic sequencing in expert backward speakers, *Sci. Rep.* 10 (1) (2020) 1–17.
- [21] R. Henson, R. Henson, C. Büchel, O. Josephs, K. Friston, The slice-timing problem in event-related fMRI: the slice-timing problem in event-related fMRI, *Neuroimage* 9 (1999) 125.
- [22] Y. Behzadi, K. Restom, J. Liu, T.T. Liu, A component based noise correction method (CompCor) for BOLD and perfusion based fMRI, *Neuroimage* 37 (1) (2007) 90–101.
- [23] S. Whitfield-Gabrieli, A. Nieto-Castanon, Conn: a functional connectivity toolbox for correlated and anticorrelated brain networks, *Brain Connect.* 2 (3) (2012) 125–141.
- [24] J. JY, P. CA, L. YB, K. CK, Investigation of functional connectivity differences between voluntary respirations via mouth and nose using resting state fMRI, *Brain Sci.* 10 (10) (2020).
- [25] K.J. Worsley, S. Marrett, P. Neelin, A.C. Vandall, A unified statistical approach for determining significant signals in images of cerebral activation, *Hum. Brain Mapp.* 4 (1) (1996) 58–73.
- [26] J. Chumbley, K. Worsley, G. Flandin, K. Friston, Topological FDR for neuroimaging, *Neuroimage* 49 (4) (2010) 3057–3064.
- [27] G. Chen, P.A. Taylor, R.W. Cox, Is the statistic value all we should care about in neuroimaging? *Neuroimage* 147 (September) (2017) 952–959.
- [28] S. Brodoehl, C. Gaser, R. Dahnke, O.W. Witte, C.M. Klingner, Surface-based analysis increases the specificity of cortical activation patterns and connectivity results, *Sci. Rep.* 10 (1) (2020) 1–13.
- [29] J. Pajula, J. Tohka, Effects of spatial smoothing on inter-subject correlation based analysis of fMRI, *Magn. Reson. Imaging* 32 (9) (2014) 1114–1124.
- [30] J. Klaus, G. Hartwigsen, Dissociating semantic and phonological contributions of the left inferior frontal gyrus to language production, *Hum. Brain Mapp.* 40 (11) (2019) 3279–3287.
- [31] P. Indefrey, W.J.M. Levelt, The neural correlates of language production, *New Cogn. Neurosci.* (2000) 845–865.
- [32] S. Wu, J. C., G. Maguire, G. Riley, J. Fallon, L. LaCasse, S. Chin, E. Klein, C. Tang, S. Cadwell, Lottenberg, A positron emission tomography 1-8F deoxyglucose study of developmental stuttering, *Neuroreport An Int. J. Rapid Commun. Res. Neurosci.* 6 (3) (1995) 501–505.
- [33] M.A. Gernsbacher, M.P. Kaschak, Neuroimaging studies of language production and comprehension, *Annu. Rev. Psychol.* 54 (1) (2003) 91–114.
- [34] J.W. Dong, N.M.P. Brennan, G. Izzo, K.K. Peck, A.I. Holodny, fMRI activation in the middle frontal gyrus as an indicator of hemispheric dominance for language in brain tumor patients: a comparison with Broca's area, *Neuroradiology* 58 (5) (2016) 513–520.

- [35] D.J. Acheson, M.C. MacDonald, Verbal working memory and language production: common approaches to the serial ordering of verbal information, *Psychol. Bull.* 135 (1) (2009) 50–68.
- [36] S.C. Schwering, M.C. MacDonald, Verbal working memory as emergent from language comprehension and production, *Front. Hum. Neurosci.* 14 (March) (2020) 1–19.
- [37] J. Sierpowska, et al., Involvement of the middle frontal gyrus in language switching as revealed by electrical stimulation mapping and functional magnetic resonance imaging in bilingual brain tumor patients, *Cortex* 99 (November) (2018) 78–92.
- [38] M.S. Koyama, D. O'Connor, Z. Shehzad, M.P. Milham, Differential contributions of the middle frontal gyrus functional connectivity to literacy and numeracy, *Sci. Rep.* 7 (1) (2017) 1–13.
- [39] J.G. Rueckl, et al., Universal brain signature of proficient reading: evidence from four contrasting languages, *Proc. Natl. Acad. Sci. U. S. A* 112 (50) (2015) 15510–15515.
- [40] S. Fresnoza, et al., Dissociating arithmetic operations in the parietal cortex using 1 Hz repetitive transcranial magnetic stimulation: the importance of strategy use, *Front. Hum. Neurosci.* 14 (July) (2020) 1–15.
- [41] J. Wen, et al., Evaluating the roles of left middle frontal gyrus in word production using electrocorticography, *Neurocase* 23 (5–6) (2017) 263–269.
- [42] M. Meyer, K. Steinhauer, K. Alter, A.D. Friederici, D.Y. von Cramon, Brain activity varies with modulation of dynamic pitch variance in sentence melody, *Brain Lang.* 89 (2) (2004) 277–289.
- [43] M. Blomgren, S.S. Nagarajan, J.N. Lee, T. Li, L. Alvord, Preliminary results of a functional MRI study of brain activation patterns in stuttering and nonstuttering speakers during a lexical access task, *J. Fluency Disord.* 28 (4) (2003) 337–356.
- [44] A.C. Etchell, O. Civier, K.J. Ballard, P.F. Sowman, A systematic literature review of neuroimaging research on developmental stuttering between 1995 and 2016, *J. Fluency Disord.* 55 (2018) 6–45.
- [45] B.R. Buchsbaum, G. Hickok, C. Humphries, Role of left posterior superior temporal gyrus in phonological processing for speech perception and production, *Cognit. Sci.* 25 (5) (2001) 663–678.
- [46] G. WW, G. TJ, M. S, G. P, The left posterior superior temporal gyrus participates specifically in accessing lexical phonology, *J. Cognit. Neurosci.* 20 (9) (2008) 1698–1710.
- [47] A.P. Leff, et al., The left superior temporal gyrus is a shared substrate for auditory short-term memory and speech comprehension: evidence from 210 patients with stroke, *Brain* 132 (12) (2009) 3401–3410.
- [48] Y. Y, J. F, S. WT, T. LH, The role of anxiety in stuttering: evidence from functional connectivity, *Neuroscience* (2017).
- [49] A. H, M. K, R. A, The contribution of the cerebellum to speech production and speech perception: clinical and functional imaging data, *Cerebellum* 6 (3) (2007) 202–213.
- [50] J.A. Bernard, et al., Resting state cortico-cerebellar functional connectivity networks: a comparison of anatomical and self-organizing map approaches, *Front. Neuroanat.* 6 (AUG 2012) (2012) 1–19.
- [51] P. Mariën, et al., Consensus paper: language and the cerebellum: an ongoing enigma, *Cerebellum* 13 (3) (2014) 386–410.
- [52] M. CJ, A. J, S. SK, W. RJ, Functional neuroimaging of speech perception in six normal and two aphasic subjects, *J. Acoust. Soc. Am.* 106 (1999) 449–457.
- [53] K.R. Sitek, S. Cai, D.S. Beal, J.S. Perkell, F.H. Guenther, S.S. Ghosh, Decreased cerebellar-orbitofrontal connectivity correlates with stuttering severity: whole-brain functional and structural connectivity associations with persistent developmental stuttering, *Front. Hum. Neurosci.* 10 (MAY2016) (2016) 1–11.
- [54] S. Shroff, Caudate Nucleus, in: J.S. Kreutzer, J. DeLuca, B. Caplan (Eds.), *Encyclopedia of Clinical Neuropsychology*, Springer, New York, NY, 2011.
- [55] A. Braun, et al., Altered patterns of cerebral activity during speech and language production in developmental stuttering. An H2(15)O positron emission tomography study, *Brain* 120 (5) (1997) 761–784.
- [56] S. Ghosh, A. Basu, S.S. Kumaran, S. Khushu, Functional mapping of language networks in the normal brain using a word-association task, *Indian J. Radiol. Imag.* 20 (3) (2010) 182–187.
- [57] H. G, P. D, Dorsal and ventral streams: a framework for understanding aspects of the functional anatomy of language, *Cognition* 92 (1–2) (2004) 67–99.
- [58] S.L.E. Brownsett, R.J.S. Wise, The contribution of the parietal lobes to speaking and writing, *Cerebr. Cortex* 20 (3) (2010) 517–523.
- [59] D. Thoms, E.C. Caparelli, L. Chang, T. Ernst, fMRI-acoustic noise alters brain activation during working memory tasks, *Neuroimage* 27 (2) (2005) 377–386.